REPLY TO THE REVIEWER'S COMMENTS

We sincerely appreciate your thorough and thoughtful review. Many of the comments and suggestions required careful consideration and prompted substantial revisions to the manuscript. With your help we have managed to resolve several inconsistencies in the manuscript and clear out many critical points, that hindered readability. We have made every effort to address all remarks. We hope you will recognize the extent of our efforts and find our responses satisfactory.

Thank you very much again for your review.

The Authors

REPLIES TO THE COMMENTS

The reviewer's text is shown black, or replies red and planned changes red-italic. First we address the general comments and then we give replies to specific comments. We are also attaching a Supplement that will be added to a revised manuscript, and also address some of the comments.

Note that proposed changes are still subject to small changes, and not all citations are given!

The authors present an interesting methodology to model karst evolution due to flow, transport and the dissolution within a fracture network, below a fluctuating water table. Although the approach is mainly presented within a limited context of dams and reservoirs, such modeling approach could be useful in a much wider context as well. I think the paper could be a valuable contribution to the journal, it is well written and easy to follow. I have a few recommendations that would improve the text:

General comments:

1. While the individual steps of the modeling are mostly well presented, I would find useful to have an overview of the whole modeling process. In my opinion a flowchart would greatly help the methodology section. One thing I found confusing is the mixing of terms inner-outer iterations, steps - it was difficult to follow which steps happen within a single timestep etc. Using a flowchart could easily alleviate this issue, and would give a good entry point to the modelling process.

Reply: We acknowledge that the terminology was rather confusing, stemming from a bias inherent in the research process. To address this, we have abandoned the confusing notation for iteration levels. Instead, we now employ the terms ***confined flow solution, node-to-node iteration, and layer-by-layer***

iteration to more accurately describe the computational procedures. Additionally, we have included a flowchart Figure R1 that provides a comprehensive overview of the entire simulation workflow.

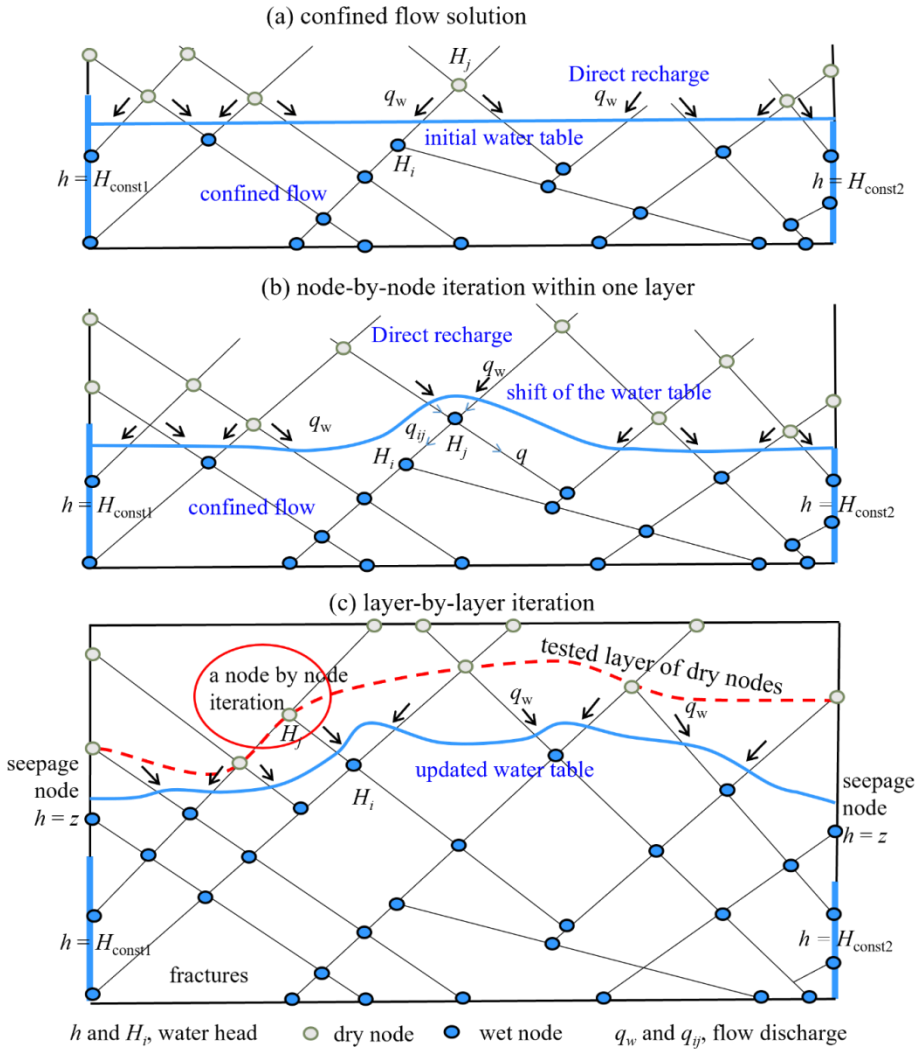

Figure 3.(renumbered) *Conceptual presentation of flow calculation in the fracture network. (a) Boundary conditions for Confined flow calculation performed at* ***every*** *iterative step. (b) Node by node iteration: testing wetting of a dry node across a layer. (c) Layer by layer iteration. H_i and H_j are heads at wetted nodes, q_w is direct recharge from the vadose flow, z is elevation of the node.*

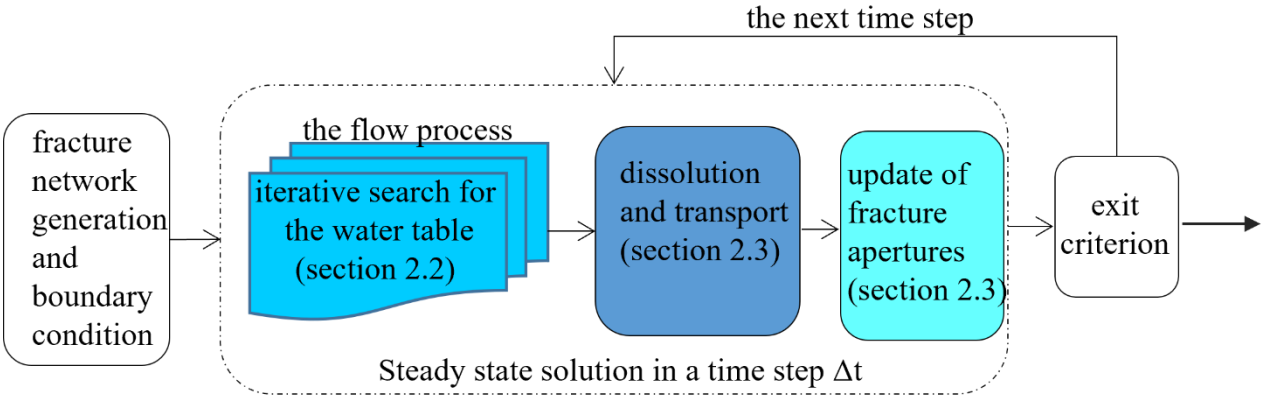

Figure R1. *The flowchart of the whole modelling process. At each time step, the new position of the water table is determined through an iterative process. Subsequently, the coupled flow, dissolution, and transport equations are solved at both the individual fracture scale and the fracture network scale. Based on these results, the fracture apertures are updated accordingly. The modified fracture network then serves as the basis for calculations in the following time step.*

2. How would you validate such modeling approach? Do you see a potential to compare the results with field measurements? Or did you consider validating the individual modelled processes against other modeling approaches? I think such validation would be an important step for presenting such new methodology. It would also be interesting to see, how the modeling results compare against other methods (such as equivalent porous media, or a static DFN model).

Reply: We agree that the analytical solution presented is not sufficient for the flow validation. Actually the analytical solution is based on Dupuit approximation, which neglects vertical flow and seepage face. We have now used MODFLOW and its DRAIN module to test the validity of our solution on some basic cases and moved the test results to Supplements.

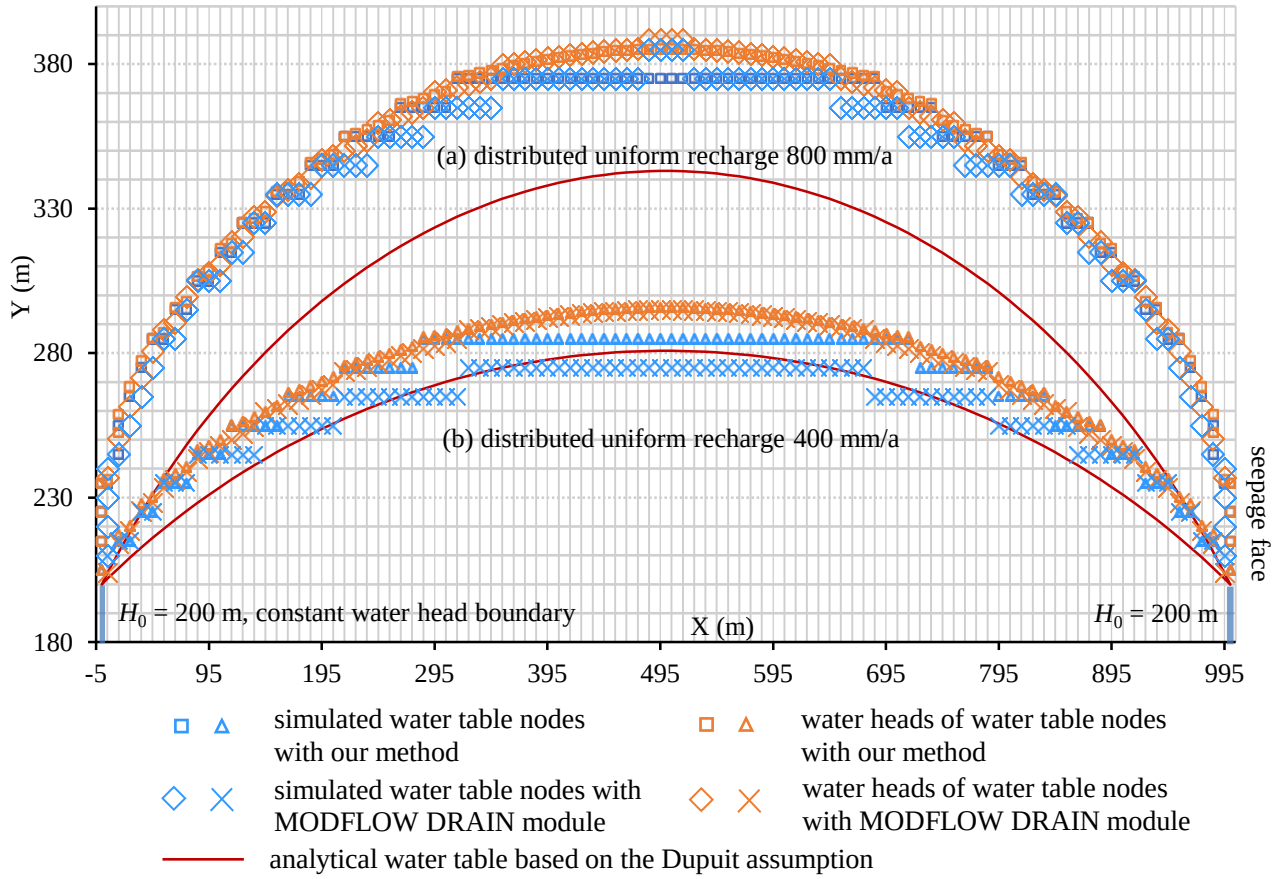

Figure S2. Water tables and corresponding heads validation with MODFLOW and Dupuit analytical approximation for two distributed uniform recharge conditions.

The accuracy of confined flow solution is assured by water head and flow balance tolerance (H_{tol} = 10^{-4} m and Q_{tol} = 0.1 cm^2/s). The flow solver uses preconditioned conjugate gradient approach for sparse matrix.

3. In general, I think there are too many figures in the manuscript, and many of them could be moved to the supplements. Fewer figures with less information, would better highlight the interesting results from the modeling.

Reply: We agree with the suggestion. The model testing section (2.4.1) and the detailed calculations from Section 2.3 have been moved to the Supplements. In their place, we have provided a concise summary of the workflow without delving into technical details. Readers interested in the full methodology can refer to the appendix for more information. However, we would prefer to retain Figures 10–12 in the main manuscript, as they convey essential insights into the formation of the LKB.

Specific comments

1. L30: The concept of LKB is very important for this paper, but this explanation is too short for it. Please explain it better.

Reply: Thanks for your valuable comment. We have further explained the concept of LKB in the revised manuscript (Introduction from Line 30 of the OM), that will now read:

Basic flow solutions in unconfined porous aquifers with constant recharge, suggest a relatively stagnant flow zone in water divide area (Rhoades and Sinacori, 1941; Tóth, 1962; Liang et al., 201). This also applies to fractured aquifer and can have important implication for karstification, where low flow zone may also result in less karstified zone. Such low karstified blocks have been recognised in water divide regions of real karst aquifers and proven to be effective in mitigation of leakage from reservoirs in karst areas (Yuan et al., 1993; Milanović, 2000; Xu and Yan, 2004). See Also Figure 1.

We have also *updated* Figure 1 and its caption, to introduce the LKB concept in a clearer manner:

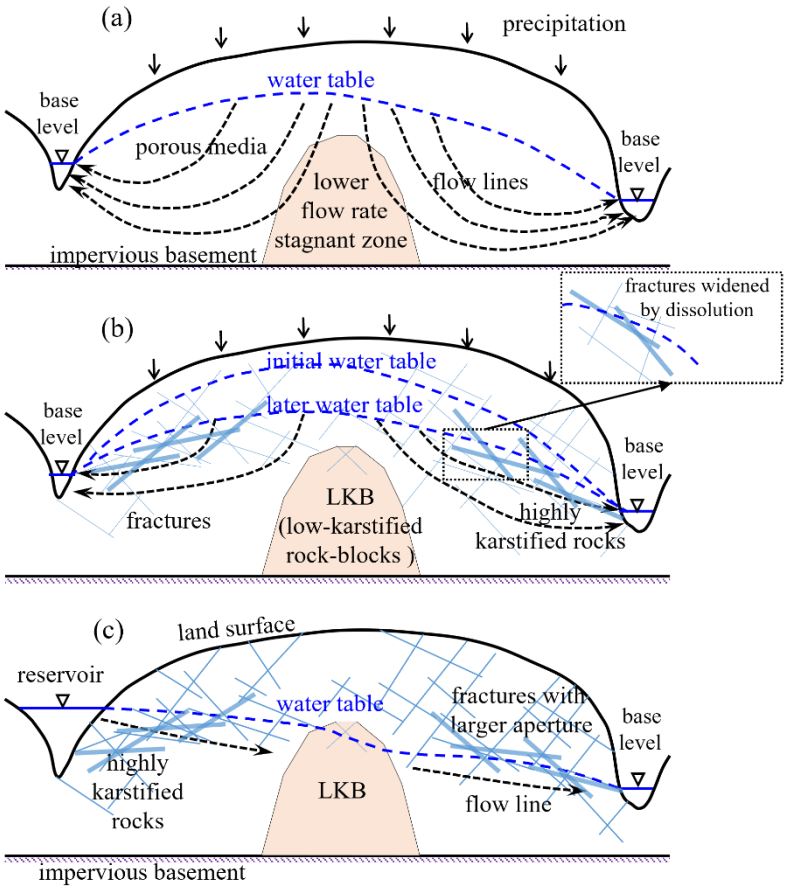

Figure 1. (a) The flow solution reveals the presence of a stagnant zone near the groundwater divide within the porous aquifer. (b) Karstification increases permeability and progressively lowers the water table over time, leading to the formation of blocks that are highly karstified and low karstified blocks (LKB). (c) When reservoirs are constructed, LKB can effectively obstruct leakage across the aquifer.

2. L35: "The pattern of groundwater flow in water divide areas also suggests the possibility of an LKB in karst aquifer." - why?

Reply: We hope that the response to previous comment also addresses this one.

3. L50 onwards: this is a very good motivation for the paper

Reply: We appreciate your feedback.

4. L90: all these steps happen within one time step

Reply: We apologize for the lack of clarity in the original presentation. We hope that the revised flow chart (Figure 2), along with the updated list in lines 91–95, now clarifies the intended workflow and structure.

5. L128: Does this mean you are aiming for a steady state within the iterations?

Reply: Yes. The system goes through a sequence of steady states. Within each time step, a stable solution for flow, dissolution and transport are found and change of fracture apertures are calculated within a time step Δt. We have made this more clear; see reply to the comment above.

6. L147: what does middle iteration mean?

Reply: Please refer to our response to General Comment 1 and the accompanying flowchart. We have revised the terminology and introduced a new flowchart to reflect these changes. See also reply to the Comment 7.

7. L149: a flowchart would be great here

Reply: We have added a flowchart of the flow calculation to the supplements, as shown below. The text in section 2.2.1 and 2.2.2 will refer to it.

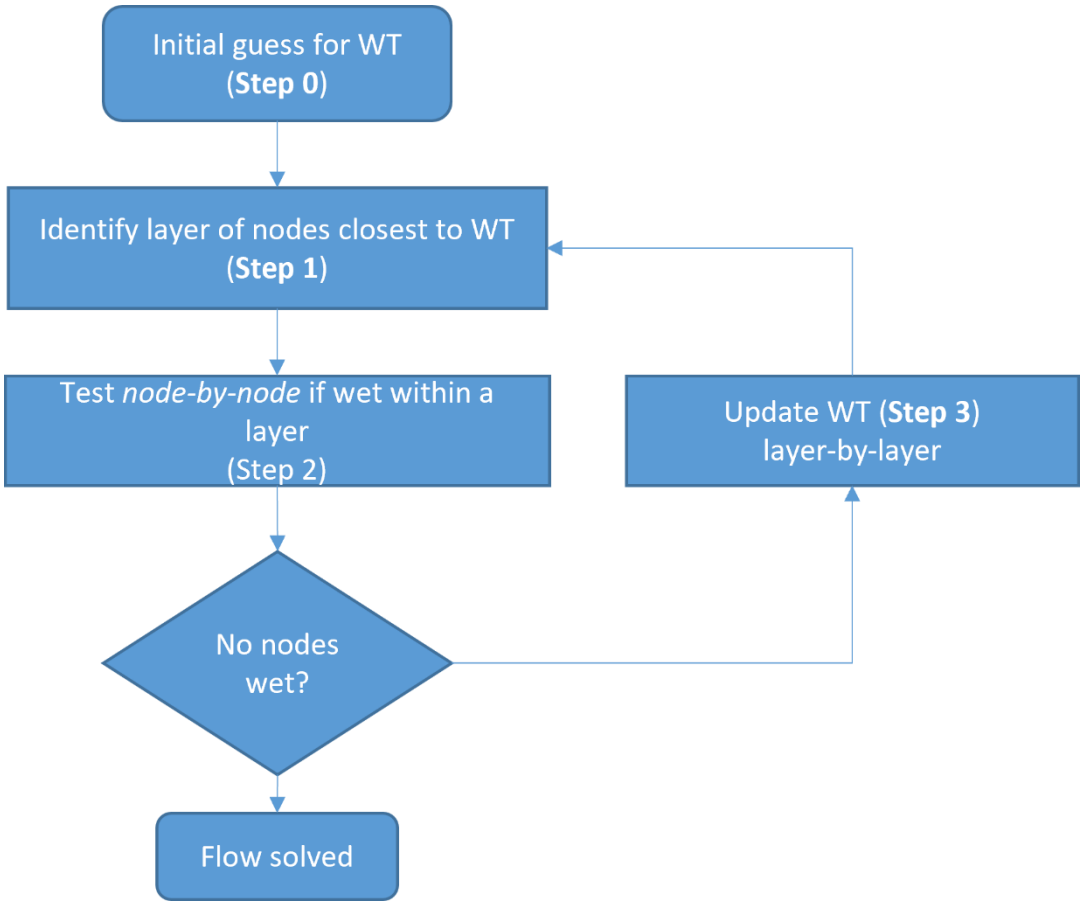

Figure R2. The flowchart of flow solution.

8. L150: What does layer-by-layer mean here? This part in general is quite confusing.

Reply: We apologize for the lack of clarity in the original submission. To address this, we have revised the caption in Figure 2 (now updated as Figure 3), introduced a new flowchart (Figure R2), added a supplementary diagram summarizing the iterative process of flow calculations (Figure R1) and changed the text correspondingly in Section 2.2.

9. L188: What does homogeneous mean here? Are you verifying against an equivalent porous media model?

Reply: Yes, "homogeneous" refers to a regular grid of fractures with a uniform aperture distribution. For such a configuration, it is straightforward to determine an equivalent porous medium with corresponding hydraulic conductivity for use in MODFLOW simulations.

10. L213: More details about the high-performance platform is needed (CPU type)

Reply: We have added the details about the computing platform to the Supplements S1, as shown below:

"The CPU type is Chinese Hygon C86 7185 32-core Processor, and the operating system is CentOS Linux 7. We use 8 cores on a single node mainly for the long time stable calculation."

11. L227: This section is unclear to me. Are we talking about in the dam or somewhere else? What is a karst reservoir in this context?

Reply: Thanks for your comment. The *reservoir* refers to a body of water behind the dam. We model the aquifer between A and B, e.g. between the reservoir on the left and the river in the right. The text will be changed clarify this aspect.

12. L235: This is a very good case study site for the approach.

Reply: Thanks for your comment. We appreciate your feedback.

13. Table 1: How did you choose the parameters?

Reply: We adopted parameters from several studies that include data from the Luojiaao interfluve aquifer. Observations of CO_2 and Ca^{2+} concentrations were collected from three boreholes and two springs. It is important to emphasize that these data are used in an illustrative manner—serving only

to loosely relate the model to a field site. The Luojiaao interfluve is presented solely as a motivating example, without any intention to construct a fully realistic or site-specific model of the system.

14. How did you choose the simulation length?

Reply: We simulated the evolution for 100,000 years, when the water table has dropped to the base level and no more dynamics is observed except for the conduit evolution at the base level. However, analysis has been made for evolution times up to 20,000 years, when the water table was in similar position as revealed by borehole data.

15. Figure 9: These plots a bit confusing, can you rotate them so the x-y plane is vertical?

Reply: We agree; sometimes authors need a kick from their bias. We have rotated the figure.

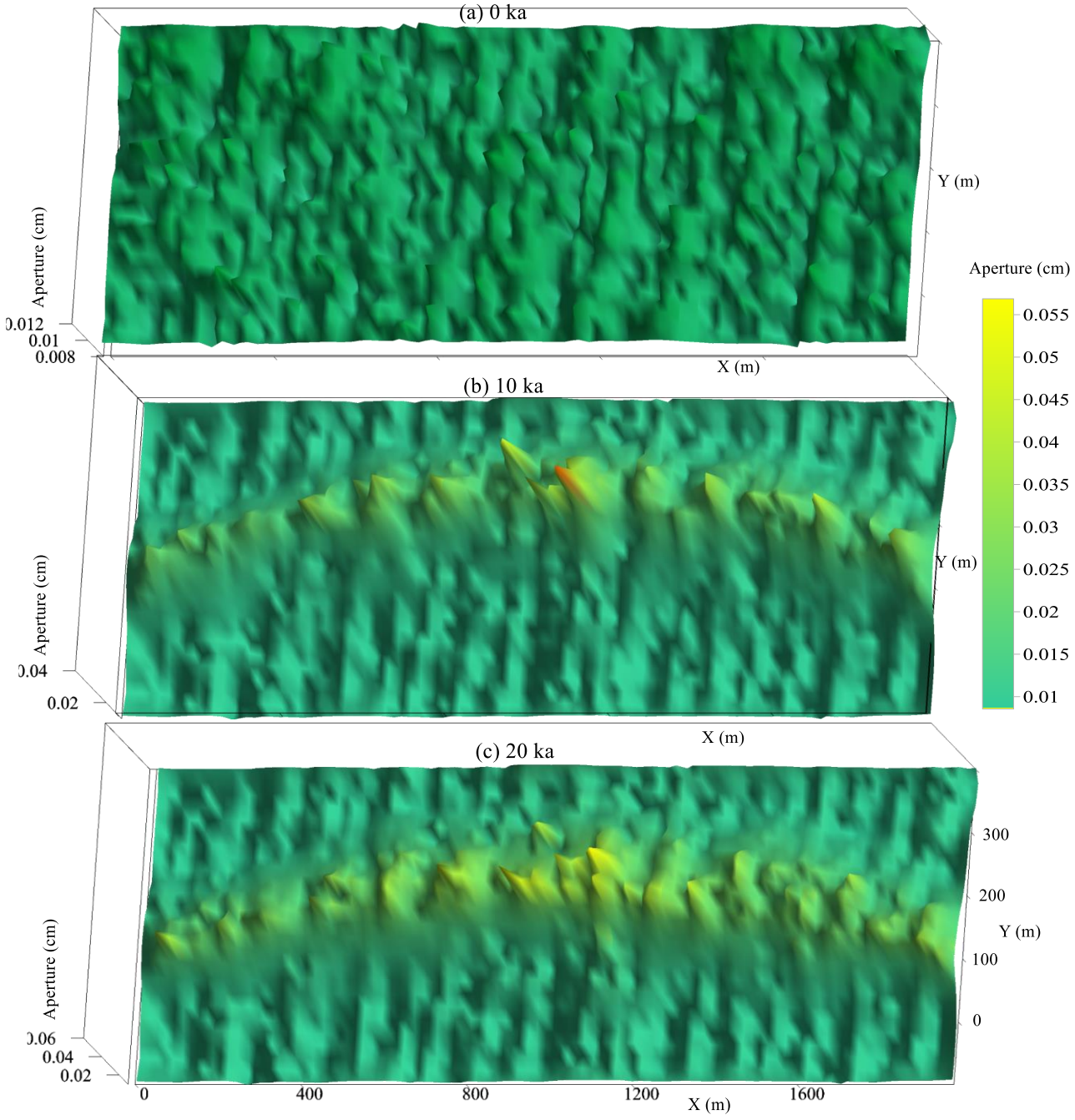

Figure 7(renumbered). Evolution of fracture aperture at 0 ka (a), 10 ka (b) and 20 ka (c) under natural conditions.

16. L272: "The water table with dissolution fringe mainly descends through the upper section, which experience the evident change in aperture" - This sentence is unclear

Reply: We agree that the sentence, as it currently stands, appears somewhat out of context. We will remove it and instead incorporate a new paragraph at the end of the section (starting from Line 285) that summarizes the underlying mechanism and conveys the intended message more clearly. The revised paragraph reads:

Karstification represents a form of nucleation, where flow-induced dissolution and changes in porosity are coupled through feedback mechanisms (Eder et al., 2021; Molins et al., 2014). *In unconfined aquifers under constant recharge conditions, dissolution is most intense near the water table. This process creates a highly permeable fringe that effectively channels inflow toward both sides of the water divide. As this fringe migrates downward across the aquifer cross-section, it leaves behind a distinctive porosity imprint. Simultaneously, it inhibits deeper penetration of the inflowing solution, favoring the preferential development of horizontal fractures. Moreover, flow along the water table increases progressively from the water divide toward the discharge points. As a result the water divide zone is less karstified than the regions close to the output. Similar anisotropic, directional changes, including fingers or preferential flows, has also been observed through experimental studies and other numerical simulations (Shavelzon and Edery, 2022; Singurindy and Berkowitz, 2003).*

17. Fig. 10-11-12: I see a lot of redundancy in these figures, are they all important? Consider moving some of them to the supplements.

Reply: We have considered avoiding the redundancy of the figures. Since we want to highlight the part of LKB formation, we would like to keep these figures. We have updated the text to refer to them.

18. L347: "Considering..." - elaborate this statement more

Reply: We have elaborated the statement. We have changed text from Line 344 to 350 that now reads:

The results show moderate and acceptable increase of leakage within the expected life span of the dam (about 100 years). However, we have to be aware that model is idealisation of reality, and that further structural, speleological and hydrological data would be required to give a more reliable site-specific prediction.

19. Where do you see here the link between the model and the real case? How could the model be used in this specific setting?

Reply: We believe that we have partially addressed this question in our previous response. However, to be sincere, real karst aquifers are extremely difficult to characterize with sufficient precision to make such predictions feasible. Nevertheless, the conceptual approach tested in this work provides valuable input for practical applications.

20. L366: this section title is unclear to me.

Reply: We have changed the title to “Concept of LKB in water divide region” We have also change title of section 5.2 to “Shortcomings of the model”.

Supplements

S1 Model details & validation

At each time step, the convergence status is recorded in the runtime output file. An example is available on our GitHub repository at Fracturetokarst2024/slurm-17392021.out.. This file includes key indicators such as the number of iterations required for solving the iterative flow equations for confined flow solver, water head errors, and total flux balance. Iterations are controlled internally both node-by-node and layer-by-layer. If the confined flow solver encounters convergence issues, the model reverts to the last successful state and proceeds by testing an the next dry node. To assess the model's accuracy, results were benchmarked against MODFLOW simulations, as described in the subsequent section.

We also explored the model's behavior under different flow regimes by simulating the coexistence of turbulent and laminar flows. These tests confirmed the numerical stability of the model. Additionally, the model is capable of generating random fractures, which are used directly in flow and dissolution computations. These fractures vary in shape and size and are not constrained by the underlying computational grid.

A high-performance computing environment is essential for achieving long-term stability in water table simulations. The calculations were performed on a platform using a Chinese Hygon C86 7185 32-core processor, running CentOS Linux 7. For these simulations, we utilized 8 cores on a single compute node.

S 2 Test of the water table in a homogeneous fractured aquifer

To verify the numerical model, we first compare the results for the homogeneous network with MODFLOW (Harbaugh et al., 2000) and the analytical solution derived using the Dupuit assumption, which can be expressed as follows:

$$H=\sqrt{H_0^2-\frac{w}{K_x}X^2+\frac{wS}{K_x}X} \tag{S1}$$

where H_0 is the river base level, K_x is the equivalent horizontal conductivity in m/d, S is the aquifer length, X is the distance from the left river boundary, and w is the intensity of rainfall recharge.

The homogeneous fracture network is shown in Figure S2.1. We assume translational symmetry and therefore use 2D domain populated by fracture. The horizontal dimension of the domain is 1000 m and vertical 400 m. The distance between the fractures in both the X direction and the Y direction is 10 m. The aperture is 0.01 cm for all the fractures. Along the two side boundaries, nodes lower than 200 m in height are given a constant water head of 200 m. Nodes above 200 m have seepage boundary conditions. The two recharge conditions were tested at 400 mm/a and 800 mm/a.

Within the MODFLOW validation, we calculate the equivalent horizontal K_x and vertical K_y by treating the aquifer as having confined water head boundaries in the X and Y directions, respectively. The conductivities are proportional to the ratio between the resulting flux and the head difference. The horizontal and vertical K values are virtually identical, both approximately 0.00705 m/d. The DRAIN module in MODFLOW was used to model the seepage face by setting each boundary node above the constant head with drainage function, which worked as its water head became higher than the drain's elevation. In Figure S2.1, water table nodes are labeled blue and the corresponding heads have orange labels. The water tables obtained via the Dupuit assumption are always lower than the simulated water table since the vertical flow and seepage face are not considered. Note that the heads at water table nodes are higher than their elevation, but below the elevation of the nearest dry node above them. The water tables simulated with our method are nearly the same as the MODFLOW simulation. Additionally, we can see the seepage face boundaries on both sides, which evidently do not exist in the analytical solution. The analysis demonstrates the effectiveness of our algorithm.

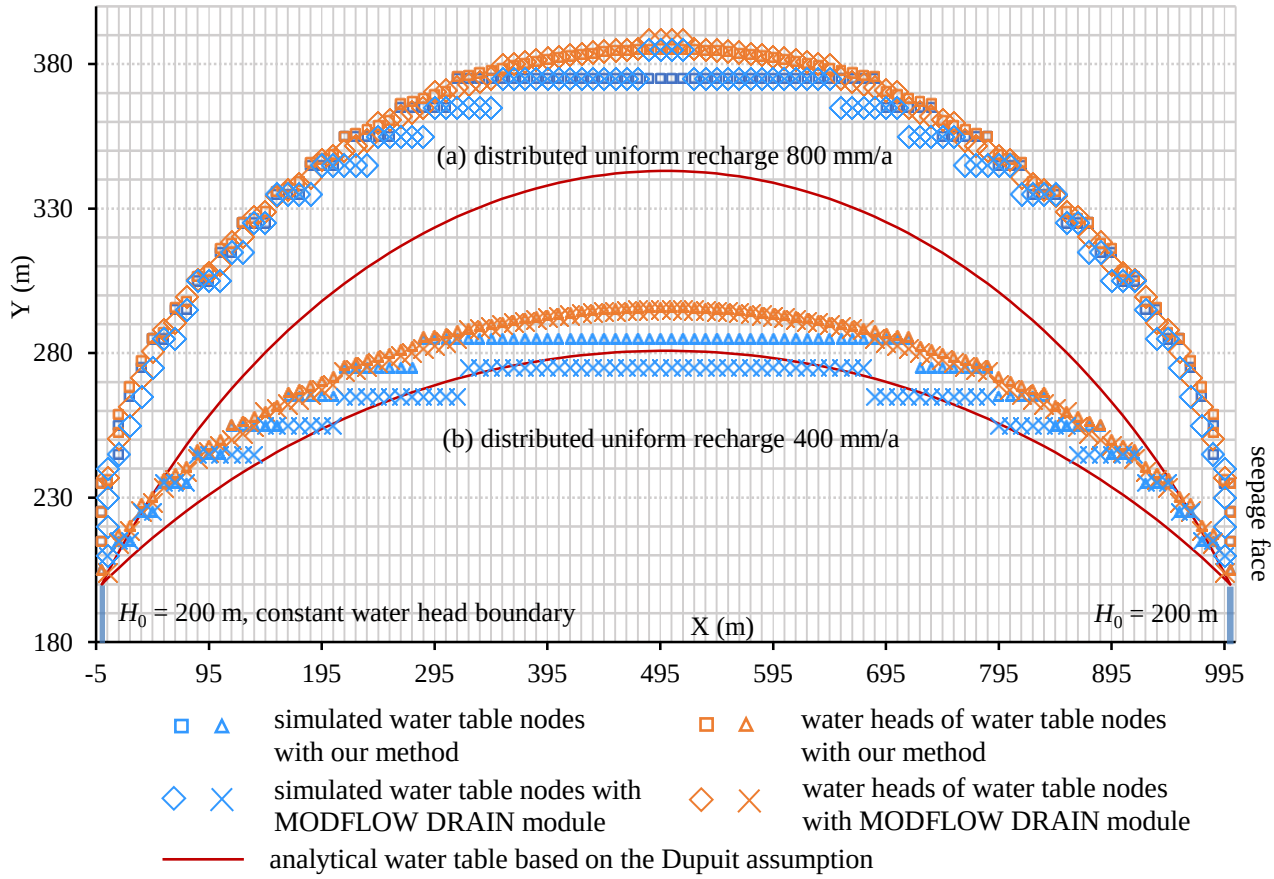

Figure S2.1: Water tables and corresponding heads validation with MODFLOW and Dupuit analytical models for two distributed uniform recharge conditions.

S3 Modeling a water table in a heterogeneous fractured aquifer

The next step is to test the solution for heterogeneous network. We use the same setting as for the homogenous network but with random generation of fractures and two recharge conditions, 200 mm/a and 400 mm/a. The equivalent horizontal and vertical K values are 0.00469 m/d and 0.00434 m/d, respectively. The number of outer iterations in all evolving time steps varied from 5 to 35. The process of searching for a water table takes approximately 3 to 4 hours during the initial modeling stages of karst evolution, and it is performed on a high-performance computing platform that utilizes 8 cores.

The fracture flow and water table data are shown in Figure S3.1 and Figure S3.2. The water table is discontinuous because of the inhomogeneous distribution of fractures. Only a few nodes for the simulated water table are lower than the analytical water table. The difference between the elevation and head at water table nodes varies due to the heterogeneity of the network. The seepage faces above the constant head boundaries on the both sides of the domain, are successfully simulated as the Signorini boundary (Jiang et al., 2013). Considering these two recharge conditions, the algorithm performed well in modelling the water table in heterogeneous network.

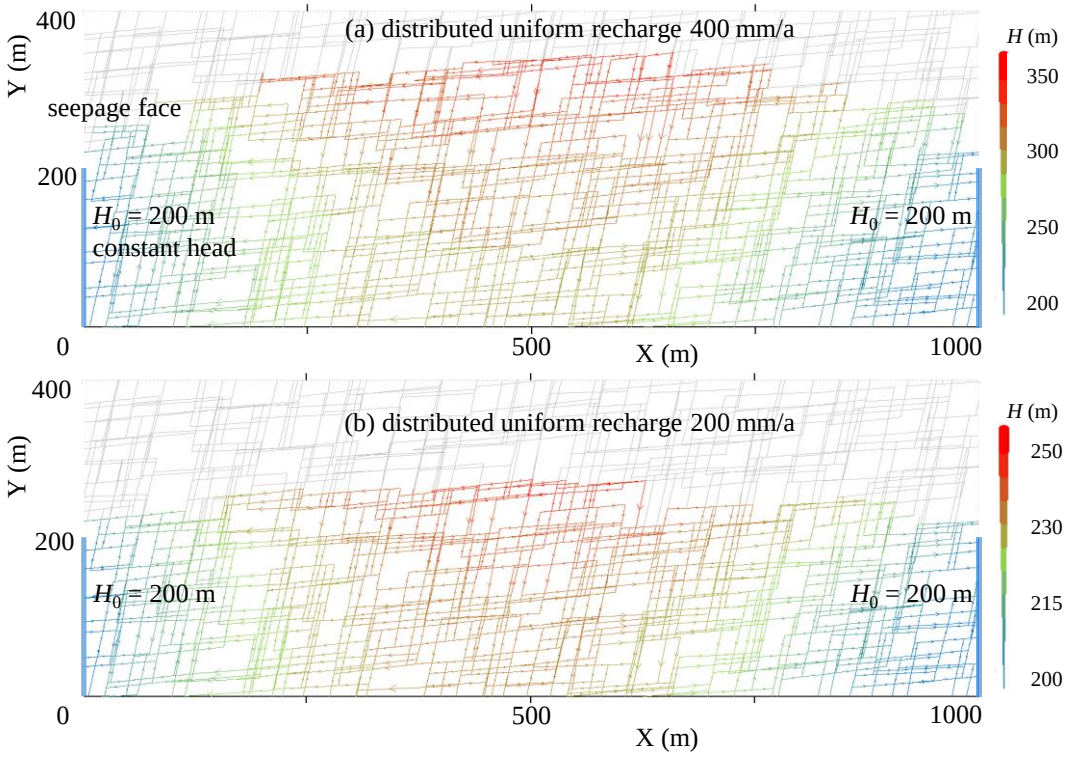

Figure S3.1. Modelling the phreatic flow in random fractures under 400mm/a and 200mm/a distributed uniform recharge conditions.

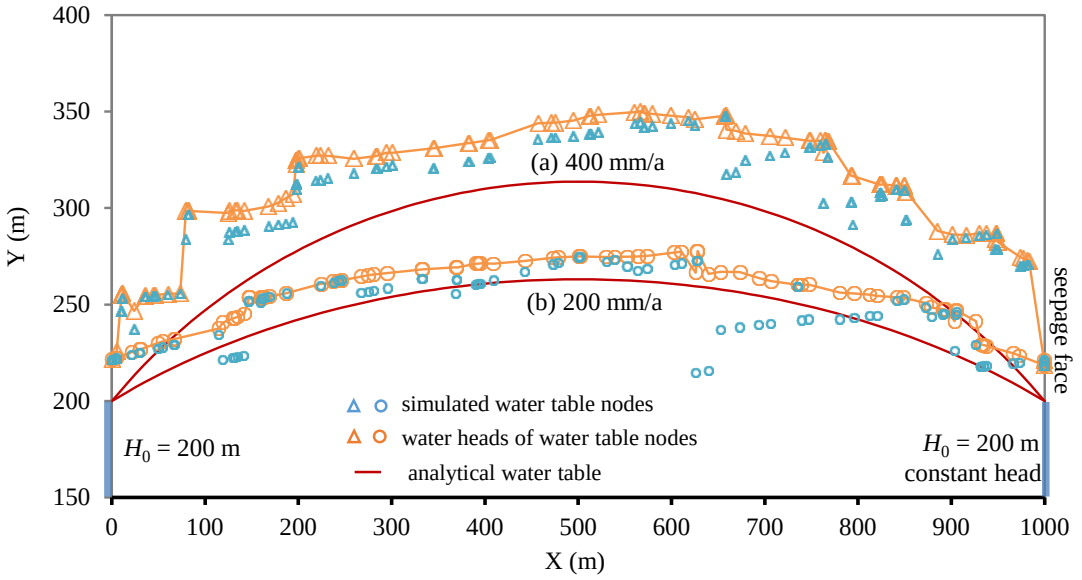

Figure S3.2: The simulated and analytical results of random fracture water tables and water heads of corresponding nodes.

S4 Changes of concentration within individual fracture and on a network scale

S4.1 Dissolution and change of concentration along an individual fracture

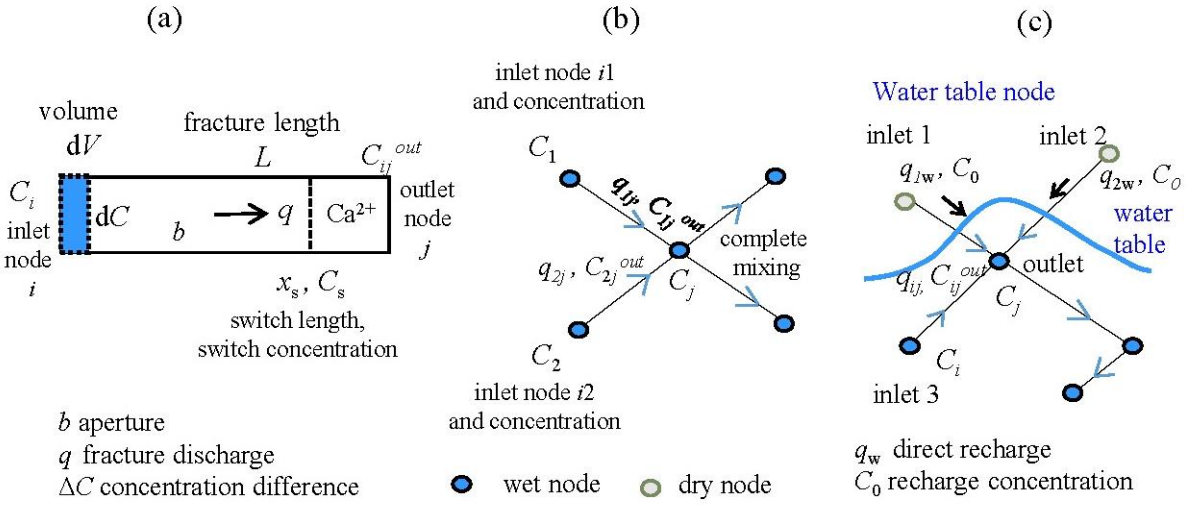

Figure S4.1: Calculating Ca^{2+} concentration along one single fracture and at fractures joint node and near the water table.

To calculate change of concentration within a single fracture, we use a Lagrangian approach and imagine a water parcel with volume $dV=Pdx$ moving along the fracture with velocity $v=Q/A$, where A is a flow crosssection, and calculate the change of concentration within the parcel (Figure S4.1). In a time dt the change of concentration in a parcel is equal to:

$$dC = F(c) \cdot P \cdot dx \cdot \ dt/dV \tag{S2}$$

Where P is flow perimeter and Pdx is the surface area of water/rock contact. Rearranging the equation gives:

$$\int_{C_i}^{c(x)} \frac{dc}{F(c)} = \frac{P}{Q}x = \frac{2(b+w)}{qw}x \approx \frac{2}{q}x \tag{S3}$$

The last term is an approximation for a wide fracture with the lateral width w and aperture b, where $w>>b$; q is flow rate per unit width. Using rate Equations (Eq. 7 and Eq. 8) for $F(c)$, we get:

$$C(x) = C_{\mathrm{eq}} - \ (C_{\mathrm{eq}} - C_i)e^{-\left(\frac{2k_1}{q\,C_{\mathrm{eq}}}x\right)}, \quad (C < C_s\,) \tag{S4}$$

$$C(x) = C_{\mathrm{eq}} - C_{\mathrm{eq}}(C_{\mathrm{eq}} - C_i)\ \sqrt[3]{\frac{q\ C_{\mathrm{eq}}}{(C_{\mathrm{eq}} - C_i)^3 6k_4 x + q\ {C_{\mathrm{eq}}}^4}}, (C_s < C < C_{\mathrm{eq}}) \tag{S5}$$

Where k_1 and k_4 are rate constants. C_{eq} and C_s are the equilibrium concentration and the switch concentration of Ca^{2+} ions.

The change of concentration ΔC at the outlet of the fracture is given by:

$$\Delta C = C_{eq} - C_{eq}e^{-\left(\frac{2k_1}{q\,C_{eq}}L\right)} + C_i\left(e^{-\left(\frac{2k_1}{q\,C_{eq}}L\right)} - 1\right), (\ C_i < C_s, x_s > L) \tag{S6}$$

$$\Delta C = C_{eq} - C_i - 0.1\ C_{eq}^2\ \sqrt[3]{\frac{q\ C_{eq}}{(0.1C_{eq})^3 6k_4 L + q\ {C_{eq}}^4}}, (C_i < C_s, x_s < L) \tag{S7}$$

$$\Delta C = C_{eq} - C_i - C_{eq}^2\ \sqrt[3]{\frac{q\ C_{eq}}{(C_{eq} - C_i)^3 6k_4 L + q\ {C_{eq}}^4}} + C_{eq}C_i\ \sqrt[3]{\frac{q\ C_{eq}}{(C_{eq} - C_i)^3 6k_4 L + q\ {C_{eq}}^4}}, (\ C_i > C_s) \tag{S8}$$

Where x_s is the switch distance of C_s. If $C_i < C_s$ and $x_s > L$, dissolved mass is calculated from Eq. (S6). If $C_i < C_s$ and $x_s < L$, Eq. (S7) is used. If $C_i > C_s$, Eq. (S8) is used for dissolved mass directly.

S4.2 Following concentration at the network scale

To assure that concentrations at the input nodes are always known, we follow the procedure of Siemers and Dreybrodt (1998) and Gabrovšek and Dreybrodt (2000). The process begins at the network's boundary nodes with the highest hydraulic heads, where head or flux values and concentrations are prescribed. Calculations then proceed sequentially along the hydraulic gradient. As illustrated in Figure S4.1(b and c), the concentration C_j at the node j is calculated using the complete mixing assumption. This involves computing the flow-weighted average of the incoming concentrations:

$$c_j = \frac{\sum_i C_{ij}^{out} q_{ij} + \sum_k C_0 q_{wk}}{\sum_i q_{ij} + \sum_k q_{wk}} \quad \text{(S9)}$$

Where q_{wk} and C_0 are flow and concentration of direct recharge at water table nodes; q_{ij} and C_{ij}^{out} are the output flow and concentration of fractures connecting nodes i and j; i sums over confined nodes that deliver flow to j, and k runs over direct input at the water table.

References

Harbaugh, A. W., Banta, E. R., Hill, M. C., and McDonald, M. G.: MODFLOW-2000, the US Geological Survey modular ground-water model: User guide to modularization concepts and the ground-water flow process, U.S. GEOLOGICAL SURVEY, Open-File Report 00-92, https://doi.org/10.3133/ofr200092, 2000.

Jiang, Q., Yao, C., Ye, Z., and Zhou, C.: Seepage flow with free surface in fracture networks, Water Resour. Res., 49, 176-186, https://doi.org/10.1029/2012WR011991, 2013.